KEK Report 84-17
December 1984
M

PERFORMANCE TESTS OF A 2-METER GRASSHOPPER MONOCHROMATOR AT PHOTON FACTORY

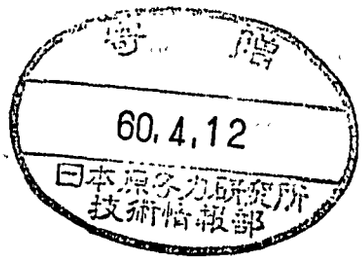

Mihiro YANAGIHARA, Hideki MAEZAWA, Taizo SASAKI,
Yoshio SUZUKI and Yasuo IGUCHI

NATIONAL LABORATORY FOR
HIGH ENERGY PHYSICS

KEK Reports are available from:

Technical Information Office
National Laboratory for High Energy Physics
Oho-machi, Tsukuba-gun,
Ibaraki-ken, 305
JAPAN

Phone: 0298-64-1171
Telex: 3652-534 (Domestic)
(0)3652-534 (International)
Cable: KEKOHO

PERFORMANCE TESTS OF A 2-METER GRASSHOPPER MONOCHROMATOR AT PHOTON FACTORY

Mihiro YANAGIHARA*, Hideki MAEZAWA, and Taizo SASAKI
National Laboratory for High Energy Physics
Oho-machi, Tsukuba-gun, Ibaraki-ken, 305 Japan
Yoshio SUZUKI**
National Laboratory for High Energy Physics
and
Department of Pure and Applied Sciences, University of Tokyo***
Yasuo IGUCHI
Insitute of Applied Physics, University of Tsukuba
Sakura-mura, Niihari-gun, Ibaraki-ken, 305 Japan

Abstract

A 2-meter grasshopper monochromator was installed and adjusted at BL-11A in Photon Factory, and performance tests were carried out. The usable photon energy range for the monochromator is 90 to 1000 eV for a 2400 grooves/mm grating, and the flux is 10^8 - 10^9 photons/sec for entrance and exit slit widths of 15 μm. A resolving power of about 2000 is realized at 250 eV for this slit width.

KEYWORDS: grazing-incidence monochromator, synchrotron radiation, concave grating, performance tests, energy region 90 - 1000 eV, photon flux, resolving power

---

* present address: Department of Physics, Faculty of Science, Tokyo Metropolitan University, Fukasawa, Setagaya-ku, Tokyo, 158 Japan

** present address: Hitachi Ltd.

*** Graduate student

1. Introduction

Using synchrotron radiation (SR) as a light source, systematic studies on the optical properties of materials in the vacuum ultraviolet (VUV) region have become possible. A monochromator usable for these studies has to satisfy requirements such as high resolution, high intensity, and ultrahigh vacuum compatibly. As a soft x-ray monochromator conformable to the PF 2.5 GeV storage ring, we introduced a 2-m grasshopper monochromator (Mark VII) from Baker Manufacturing Co., USA, last year. It was set up at station BL-11A. In this paper we will describe the installation at beam line 11A (BL-11A) and report the results of performance tests for the monochromator carried out during machine time last year.

2. Monochromator

2.1 Optics

The "grasshopper" is a sort of Vodar-type monochromator. The scanning principle was reported previously by Brown et al.[1]. It can be summarized briefly as follows: The optical system of the grasshopper monochromator is composed of a pre-mirror M_1, a plane mirror and entrance slit combination (Codling slit) S_1, a concave grating G, and an exit slit S_2, as illustrated in Fig. 1. These optical elements are shifted along a Rowland circle pivoted about the exit slit S_2. Figure 1 shows two positions of the monochromator, scanned for a wavelength λ (solid line) and for zero order light (broken line). The three elements M_1, S_1, and G translate together with the wavelength scanning. S_1 is made to direct the incident light beam onto G by the use of a half-angle mechanism. On the other hand, the distance between S_1 and G is fixed, which means $\angle S_1S_2G$ is always constant.

Therefore G translates on a fixed line, and the direction of the output light is always constant, as indicated in Fig. 1.

2.2 Scanning equation

The scanning equation of the monochromator is expressed as follows: The distance L between S_1 and S_2 is given from Fig. 1 by

$$L = R\sin(\alpha + \beta),$$

where R is the diameter of the Rowland circle, α the angle of incidence, and β the angle of diffraction. Using the grating equation:

$$\lambda = d(\sin\alpha - \sin\beta),$$

where d is the grating constant, we obtain an equation for L as

$$L = R\{\cos\alpha(\sin\alpha - \frac{\lambda}{d}) + \sin\alpha \sqrt{1 - (\sin\alpha - \frac{\lambda}{d})^2}\} \quad ,$$

As will be shown later, wavelength calibration with the above equation was carried out using results of gas absorption spectra. A change in L is equal to the change in a driving distance for the grating chamber. This distance is always monitored using a Heidenhain linear encoder attached to the grating chamber. The reproducibility of the relation between the wavelengths and L was ascertained to be high within the resolving power of the monochromator for slit widths of 15 μm.

2.3 Optical elements

a) Deflecting mirror (M_0)

SR from the storage ring is deflected by four degrees horizontally with a plane mirror M_0 located 10.8 m from the electron orbit, as indicated in Fig. 1. M_0 is a 40-cm-long silicon carbide (SiC) mirror coated with platinum. On the M_0 mirror, radiation of wavelengths longer than those for hard x-rays is selectively reflected. Thus, the VUV light beam is directed to M_1 mirror at a distance of 23.5 m from the light source. The deflecting angle and the position of M_0 are precisely adjustable using a goniometer with driving motors, the steps of which are displayed on the control panel. Although the direction of the SR beam sometimes shifts, this effect is correctable by adjusting M_0 while monitoring the output with detectors downstream from the monochromator. Details of this system will be reported by Koide (KEK) et al.[2].

b) Pre-focusing mirror (M_1)

M_1 is a concave gold-coated quartz mirror located at a distance of 23.5 m from the electron orbit. It is 30 cm in length. It images the light source onto the entrance slit S_1, 50 cm behind it. Adjustment of the focusing is made by the use of fine-adjustment screws from outside the vacuum. The angle of incidence of the light beam with respect to the surface is 2 degrees. Thus, the vertical dispersing angle of the incoming beam intercepted by M_1 is $\frac{300 \times \sin 2^\circ}{23500}$ = 0.45 milliradian. The FWHM of the vertical angular distribution of the photon flux from the 2.5-GeV PF-RING is about 0.5 milliradian in the VUV region. The radius of curvature R of the surface is obtained from

$$\frac{1}{23.5} + \frac{1}{0.5} = \frac{2}{R \cos 88°} \quad .$$

The calculated value of R is 28.1 m. The nominal value of the furnished mirror is 28 (±0.5) m. Judging from the carbon-contamination pattern imaged on the holder of the Codling slit, good focusing by the M_1 mirror is realized.

c) Entrance and exit slits (S_1 and S_2)

S_1 is a mirror-slit combination. The mirror is a gold-coated planar quartz blank.

The grazing angle of the incident light with respect to the surface changes from 3° to larger angles for a wavelength scan from zero order to longer wavelengths. This is effective not only in maintaining high reflectivity at shorter wavelengths, but in suppressing high-energy higher-order light at longer wavelengths.

Initial adjustment of the minimum slit width was carried out cautiously. The slit width is adjustable in situ from a few μm to 400 μm by using a linear feedthrough with a micrometer. The change velocity of the slit width is 4 μm per smallest division of the micrometer (10 μm). We always move the micrometer from higher to lower numbers to avoid backlash.

The mirror of the Codling slit has a tendency to be contaminated with carbon along the slit edge, on account of the intense focusing. But the contamination rate has recently been much lower than it was before owing to the lower pressure of the monochromator. If the mirror is contaminated after some beam time, we rotate it in the surface plane by some degrees to avoid the contaminated area. The minimum width of the mirror-slit S_1 is also adjustable by a set of screws pressing the mirror surface against the slit jaw. The adjustment should be done cautiously so that the jaw

will not touch the mirror surface, and that the two are parallel with each other.

The width of the exit slit S_2 can be controlled in situ from zero to 300 μm by the use of an external micrometer. The actual slit width was ascertained to be linear with the micrometer readings (2.0 μm/smallest division) using a microscope.

d) Grating (G)

Our Mark VII grasshopper has been designed for use with a 2-m concave grating at an incidence angle of 88 degrees. The mounted grating is a 2400 grooves/mm gold-coated replica made by Hitachi Co.. It has the following specifications.

Blank size	:	$45 \times 35 \times 10$ mm^3
Ruled area	:	35×35 mm^2
Radius	:	1999.5 mm
Groove density	:	2400 ℓ/mm
Blaze angle	:	1.75°

The blaze wavelength for this case is about 17 Å, which is in the shorter wavelength region for this monochromator, as shown later.

We exchange gratings every 300-500 hours, if the output level in the short wavelength region becomes lower than half of the initial value.

e) Optical filter

In order to suppress stray and higher order light, 0.2, 0.37, and 1.0-μm-thick self-supported films of aluminum are employed behind a refocusing mirror, as illustrated in Fig. 2. The filters were made in the following way: The metal is evaporated and deposited onto a collodion film supported by a slide glass in an evaporation chamber. The evaporation was carried out as fast as possible (∿ 5 seconds). The evaporated glass was

dipped into isoamyl acetate, and the metal film was detached from the glass. It was then picked up on a 10-mm-I.D. nickel mesh supported by an aluminum holder. The 1.0 μm filter has proved to be effective in the energy region between 500 and 1000 eV.

2.4 Optical alignment

At first, adjustment of the monochromator was carried out before installation using a laser beam . It was then installed at the BL-1A station using a transit and an automatic level. Fine alignment of the optical elements was performed using the visible SR light beam coming through a glass window attached to the separation chamber before the monochromator (see Fig. 2). Adjustments for M_0 and M_1 were made as mentioned before. The surface position of the grating was adjusted with precise screws on the grating holder so that the incident light spot was centered on it. The zero order position of the monochromator was adjustable from outside the vacuum by means of an arm and a micrometer attached to the grasshopper's leg (see Fig. 2). By monitoring the output intensity of a photomultiplier 1P21 attached behind the exit slit S_2, the angle and position of the elements M_0, M_1, S_1, and G were finally adjusted .

2.5 Coupler

Here we report an improvement made to the monochromator. The trouble was that an oscillatory pattern appeared in every spectra when the monochromator was scanned. Its period was that of the rotation of the pulse motor installed to drive the ball-screw. Lateral motion of the ball-screw, which was slightly bent, caused an oscillation of the grating chamber on the order of 10 μm. In order to supress the oscillation, we exchanged the coupler

between the ball-screw and the grating chamber with a new one, as illustrated in Fig. 3. The vertical force due to the ball-screw deviation from straightness was reduced with two ball-bearings in this coupler. With it, the oscillatory pattern in the spectra was almost completely eliminated.

3. Refocusing mirror

The direction of the outcoming beam from the exit slit (two degrees upward) is made horizontal using a refocusing mirror installed 560 mm behind the exit slit S_2. In addition,using a bending mechanism, focused, parallel, or a dispersed light flux can be easily obtained. Details of the mirror system will be reported elsewhere, but can be summarized briefly as follows: 1) the bendable mirror is a platinum-coated 220-mm long planar Pyrex slab, 2) the vertical size of the image focused near samples is about 0.1 mm, and 3) a vacuum level of 1×10^{-9} Torr is realized after baking at 200°C for 12 hours. About half of the beam is intercepted by the mirror. Focusing by the mirror has proved to be good, as indicated by soft x-ray reflectance measurements carried out by Yanagihara et al.[3]. On the other hand, horizontal focusing can not be accomplished using the installed planar mirror, because of the grazing incidence angle. Thus, the usable beam is 0.2 milliradian in horizontal dispersion, when horizontal beam size at the sampl is 4.5 mm.

4. Light-intensity monitor

A monitor for the incident light intensity is installed behind the refocusing mirror, as illustrated in Fig. 2. It is composed of a CuI-evaporated photocathode and a head-on type 16-dynode electron multiplier,

type R660 (Hamamatsu Photonics Co., Ltd.), as illustrated in Fig. 4. CuI was employed as a high-photoelectric yield material. In addition, the photocathode is shaped to collimate the light beam horizontally, as shown in Fig. 4. The horizontal beam size can easily be controlled from 0 to 6.5 mm by raising or lowering the photocathode with a linear motion feedthrough. The electrons ejected from the photocathode are captured and amplified by the R660. The signal from the R660 is detected using a pulse-counting system, as illustrated in Fig. 5.

5. Evacuation system

The monochromator is mainly evacuated using a 500-ℓ/sec ion pump positioned under the separation chamber as illustrated in Fig. 2. In addition, a Varian 30-ℓ/sec ion pump is attached to the top of the grating chamber to improve the vacuum level around the grating and the Codling slit. The monochromator is also evacuated using a 140-ℓ/sec ion pump under the refocusing-mirror chamber through a 36-mm I.D. bellows. The monochromator is generally baked out at 60-100°C for 30 hours, while the ion pumps are baked at higher temperatures. A vacuum of 4×10^{-9} Torr is achieved in the exit slit region, hence the vacuum level in the grating chamber is better.

6. Performance tests

6.1 Photon flux

A spectrum of the monochromatized output behind the exit slit of the monochromator was obtained by observing the total photoelectric yield of CuI mounted as a photocathode on a 20-dynode electron multiplier, type R595 (Hamamatsu Photonics Co., Ltd.). The spectrum is shown by a solid curve in Fig. 6 as a function of photon energies between 100 and 1100 eV. The energy

was calibrated as will be described later. Although the yield of CuI is not constant with photon energy, this spectrum indicates the general features of the photon flux spectrum. Figure 7 shows the spectrum obtained by use of a gold mesh and a Ceratron (Murata Manufacturing Co., Kyoto), located behind the exit slit of the monochromator. A large peak appears at about 700 eV (~ 17 Å) in the two spectra. The blaze angle of 1°45' for the grating yields a blaze wavelength of 17 Å at an incidence angle of 88 degrees. Therefore, the large peak is due to the blaze effect of the grating. The reduction of the photon flux in the energy region below 700 eV is due to the smaller number of photons in SR in the longer wavelength region. On the other hand, its reduction in the higher energy region above 700 eV is due to the lower reflectance of the mirrors. A large and a small dips are found at 280 and 540 eV. They correspond to the carbon and the oxygen K-edge absorptions, respectively. The dips result from photo-absorption by contamination on the mirror elements. The reduction at the carbon K-edge reaches about 50 %. Dominant structures are seen at about 650 and 950 eV in the CuI yield spectrum. These correspond to the iodine $M_{4,5}$ and the copper $L_{2,3}$-edges, respectively.

The ratio between stray or higher-order light and the primary monochromatic photon flux was ascertained to be < 5 % in the energy region below 300 eV by means of a photoelectron energy analysis for neon gas using a cylindrical mirror analyzer[4]. The ratio in the higher energy region can be shown in Fig.6 by a straight line, which is extrapolated from the curve in the further high energy region.

The photon flux at a wavelength of 50 Å from the exit slit (15 μm) was estimated to be 10^8 - 10^9/sec for a stored electron current of 100 mA using an Al_2O_3 NBS photodiode.

There is an aging effect in the reflecting elements. The broken curve in Fig. 6 is the CuI total yield spectrum observed after 300 hours from the time when the previous spectrum (solid curve) was observed. The general feature to note is that the reduction in the photon flux is proportional to the photon energy. The result is reasonable, because absorption or scattering of light from the mirror elements increase with increasing photon energy because of contamination or damage.

6.2 Resolving power

In order to test the resolving power and to calibrate the energy of the monochromator, we measured photo-absorption of several gases contained in a gas cell using an R595 and a pico-ammeter. Figures 8 and 9 show the absorption spectra of the argon $L_{2,3}$ (0.8 Torr) and the krypton $M_{4,5}$ (0.4 Torr) for a slit width of 15-15 μm. The spectral band pass is shown in the each figure. One can see small but distinguishable peaks due to the transitions from the $L_{2,3}$ to the 5d level in argon. Also, in krypton small peaks corresponding to the transitions from the $M_{4,5}$ to the 9p level are distinguishable. Figure 10 shows the K-shell absorption spectrum of oxygen gas (0.8 Torr) for a slit width of 3-3 μm. The 3 μm width was realized by monitoring the signal of the ammeter. The spectral band pass for the slit is shown in the figure. On account of the narrow band pass the structure near 540 eV can be recognized as two split peaks, assigned to the transitions of a 1s electron to the higher valence orbitals. It is due to the high-intensity photon flux that the high resolving power is realized for the

3 μm slit. Furthermore, for this slit width, the first peak in the neon K-edge absorption at about 867 eV was observed to split.

The resolving power of the monochromator can be estimated by comparing the FWHM of an absorption peak with its natural width. Here we regard the FWHM of peaks in the electron-energy-loss spectra as the natural widths[5,6]. For instance, the resolving power at 250 eV is estimated to be 2×10^3 from the argon absorption spectrum. This value is in agreement with the calculated one. Other values estimated from the oxygen and the krypton absorption spectra are also shown in Fig. 11. The broken line indicates the calculated values for a 15-15 μm slit width. But the value for oxygen was estimated from the spectra for a 3-3 μm slit width, therefore the error of the estimation was large. On the other hand, the resolving power of the monochromator decreases in the longer wavelength region because of off-focusing. Thus it is reasonable that the resolving power observed at the krypton $M_{4,5}$-edge is lower than the calculated one.

7. Summary

The following results of the performance tests for the 2-m grasshopper monochromator were ascertained:

1) The photon energy region of the monochromator is between 90 and 1000 eV for a 2400 grooves/mm grating.
2) The number of the outcoming photons at 250 eV is 10^8 - 10^9/sec for a slit width of 15-15 μm at an electron current of 100 mA.
3) The stray light level below 300 eV is less than 5%.
4) The resolving power for a slit width of 15-15 μm is about 2000, which is in fair agreement with the calculated value.
5) A vacuum of 4×10^{-9} Torr is realized.

References

1) F. C. Brown, R. Z. Bachrach and N. Lien : Nucl. Instrum. & Methods 154 (1978) 73.

2) T. Koide, S. Sato, H. Fukutani, H. Noda, S. Suzuki, T. Hanyu, T. Miyahara, S. Nakai, I. Nagakura, A. Kakizaki, H. Maezawa, T. Ohta and T. Ishii: to be submitted to Nucl. Instrum. & Methods.

3) M. Yanagihara, T. Koide, M. Niwano, T. Miyahara, S. Sato, Y. Iguchi and T. Sasaki: Photon Factory Activity Report (1982/83) VI-78.

4) T. Sasak., T. Oda and H. Sugawara : Anl. Optics 16 (1977) 3115.

5) G. C. King, M. Tronc, F. H. Read and R. C. Bradford : J. Phys. B : Atom. Molec. Phys. 10 (1977) 2479.

6) A. P. Hitchcock and C. E. Brion : J. Electron Spectrosc. Relat. Phenom. 17 (1979).

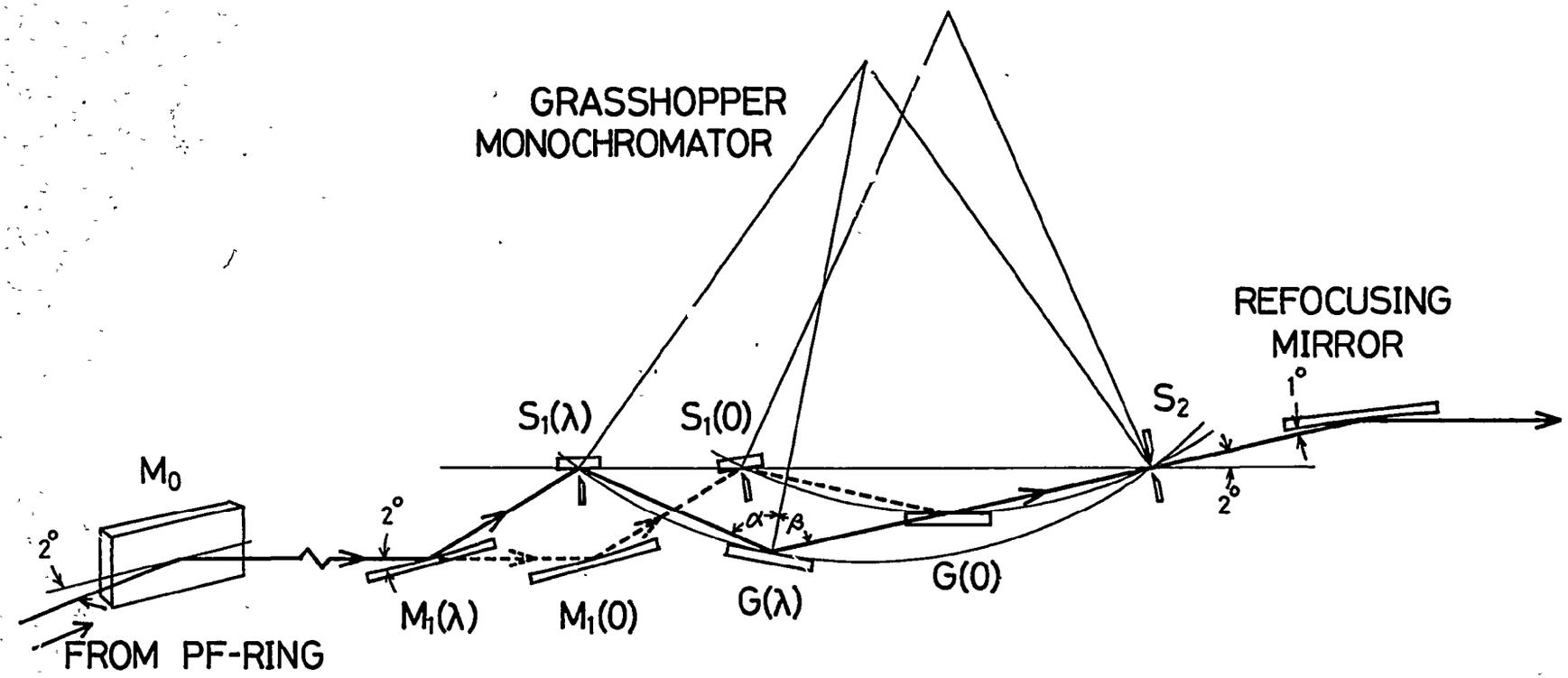

Fig. 1 Basic arrangement of optical elements for the grasshopper monochromator. M_0: deflecting mirror, M_1: pre-focusing mirror, S_1: mirror-slit combination (Codling slit), G: concave grating, and S_2: exit slit. Two positions are shown schematically, zero order and a wavelength λ.

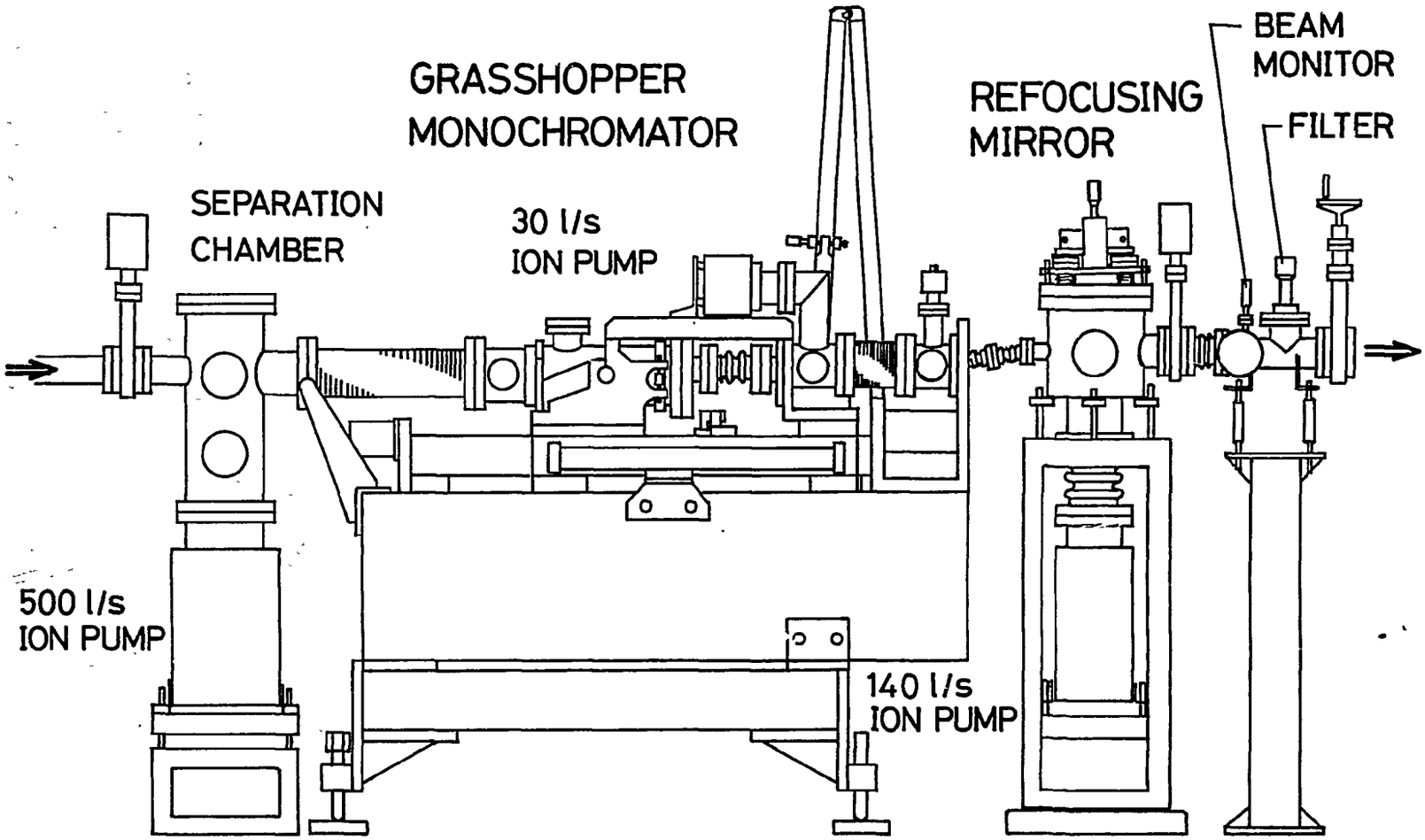

Fig. 2 - Block diagram of the grasshopper monochromator and related appara-

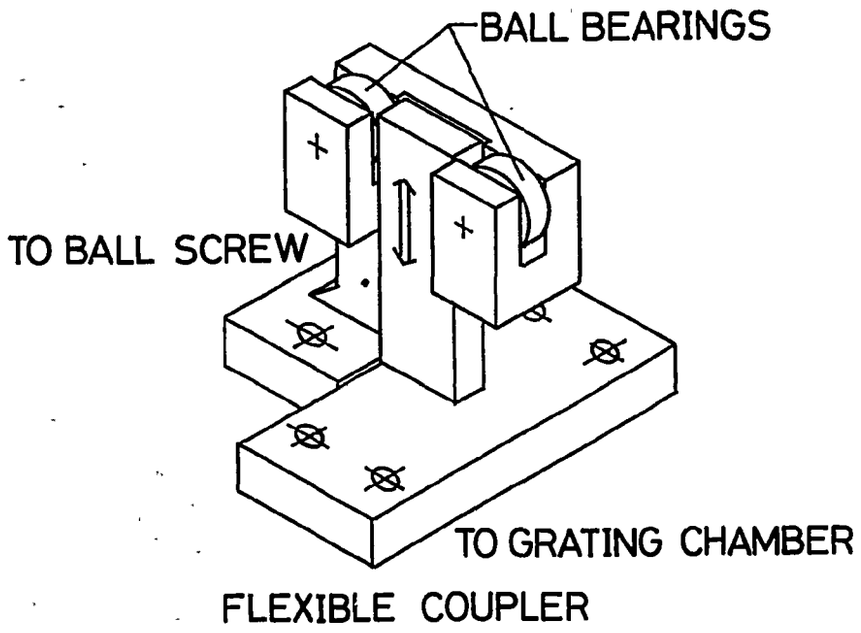

Fig. 3 Block diagram of the coupling mechanism between the ball-screw and the grating chamber.

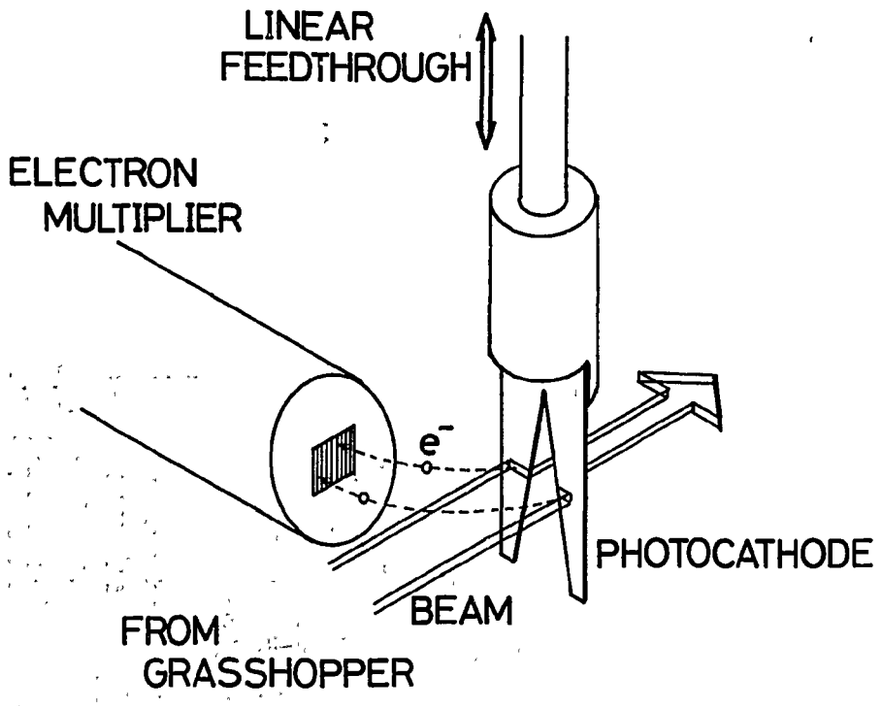

Fig. 4 Schematic diagram of the beam monitor.

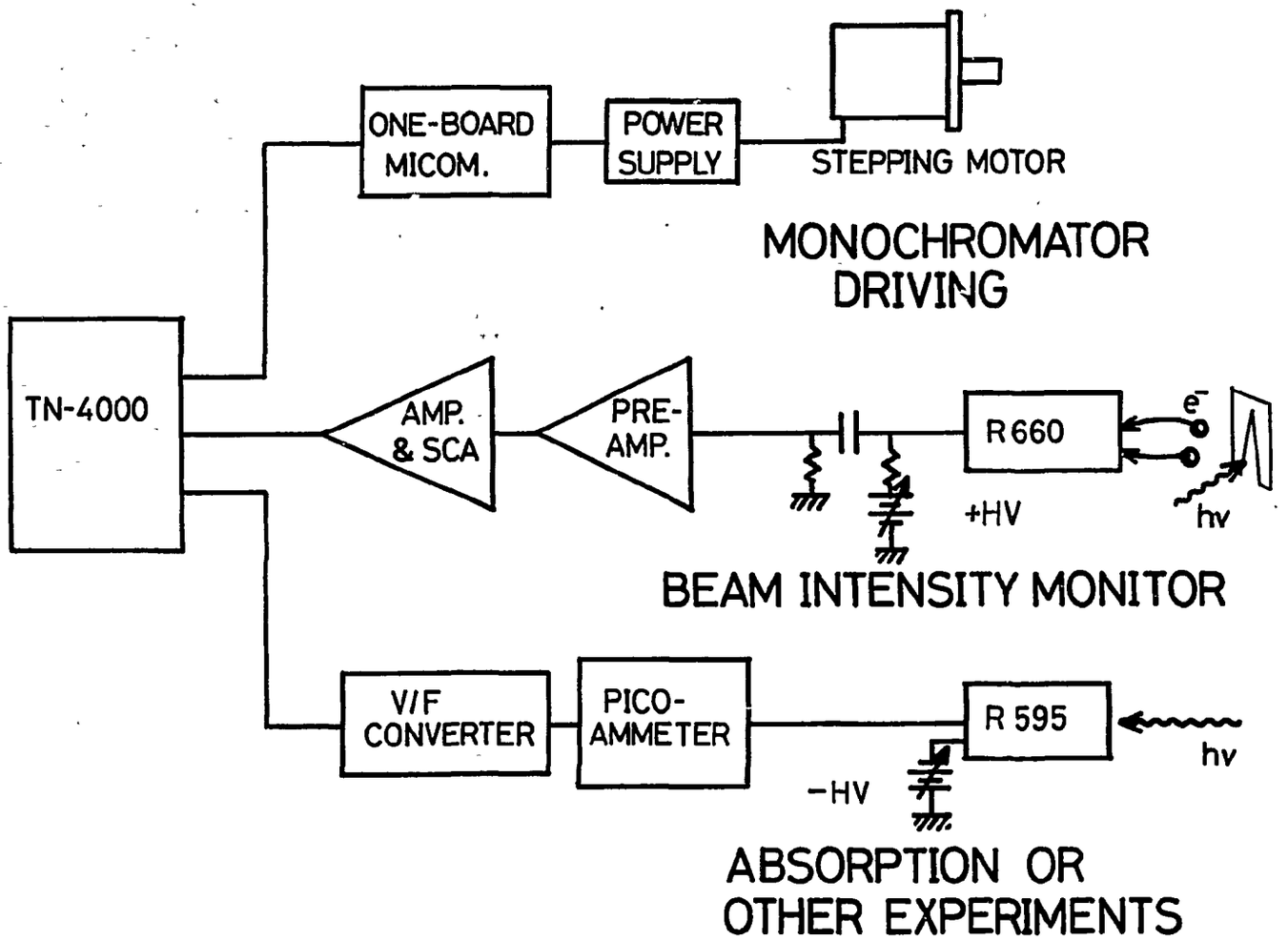

Fig. 5 Block diagram of the data taking system

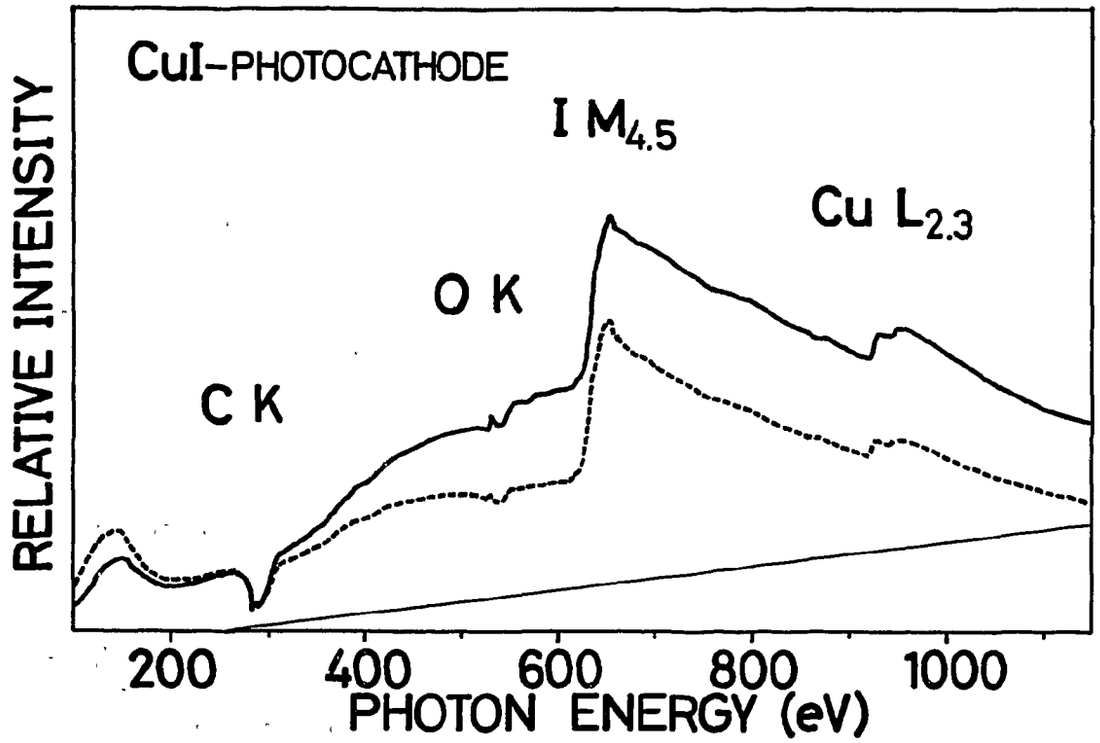

Fig. 6 Relative output intensity at the exit slit of the monochromator measured with a CuI photocathode. Two curves are shown, initial (solid) and after 300 hours (broken).

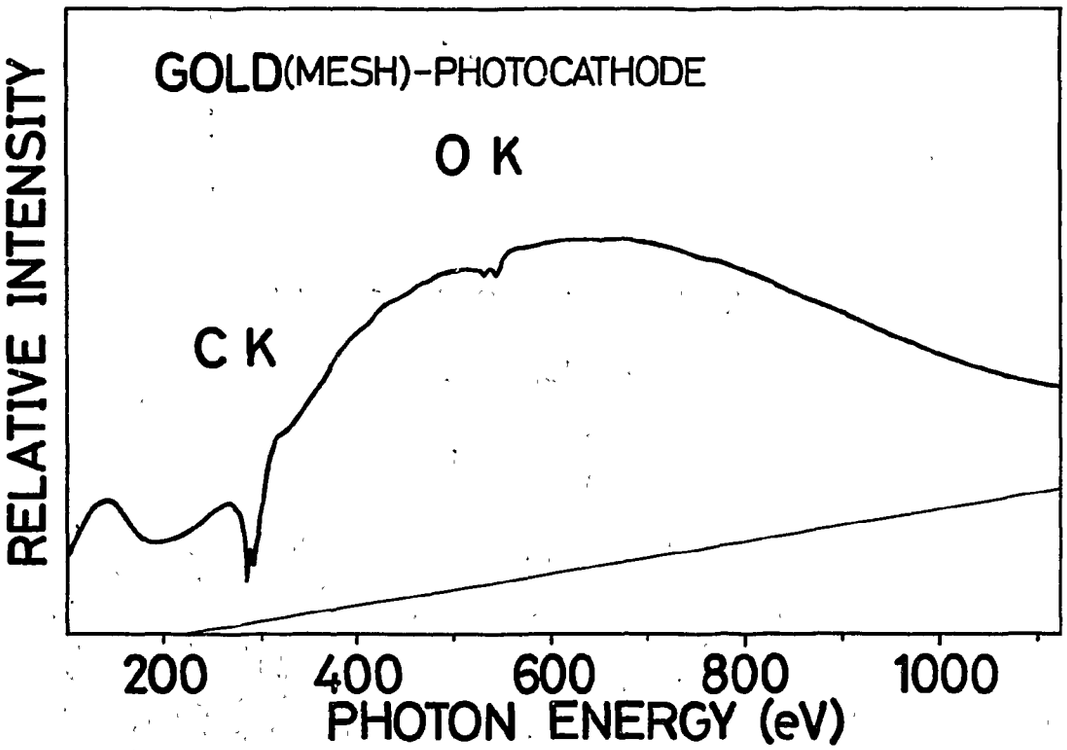

Fig. 7 Relative output intensity vs. photon energy measured with a gold mesh and a Ceratron.

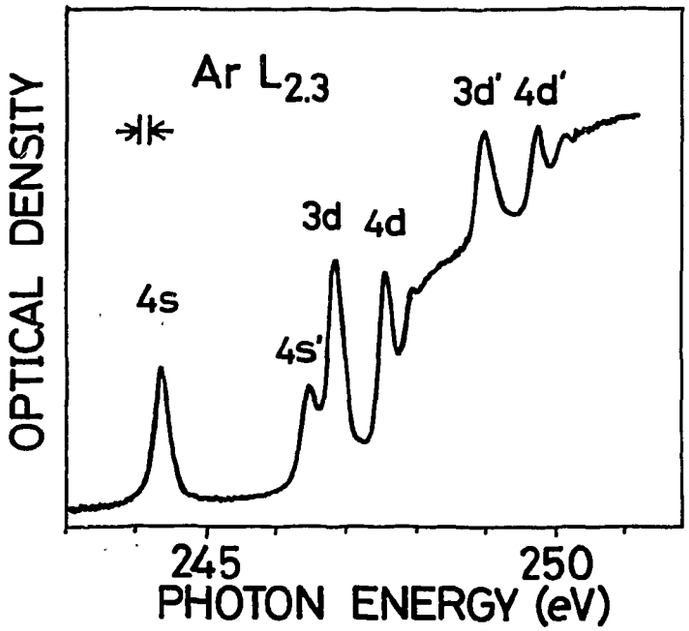

Fig. 8 Absorption spectrum of the Ar $L_{2,3}$ edge for 0.8 Torr argon gas with a 2400 lines/mm grating.

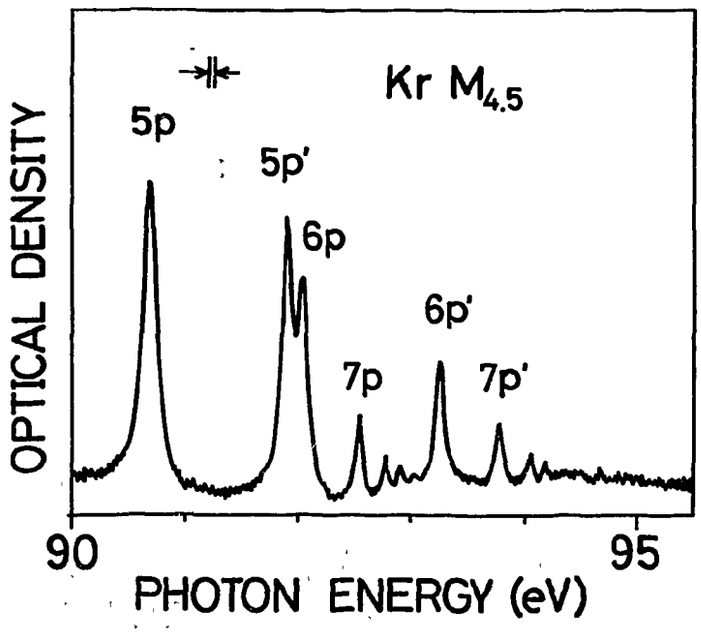

Fig. 9 Absorption spectrum of the Kr $M_{4,5}$ edge for 0.4 Torr krypton gas.

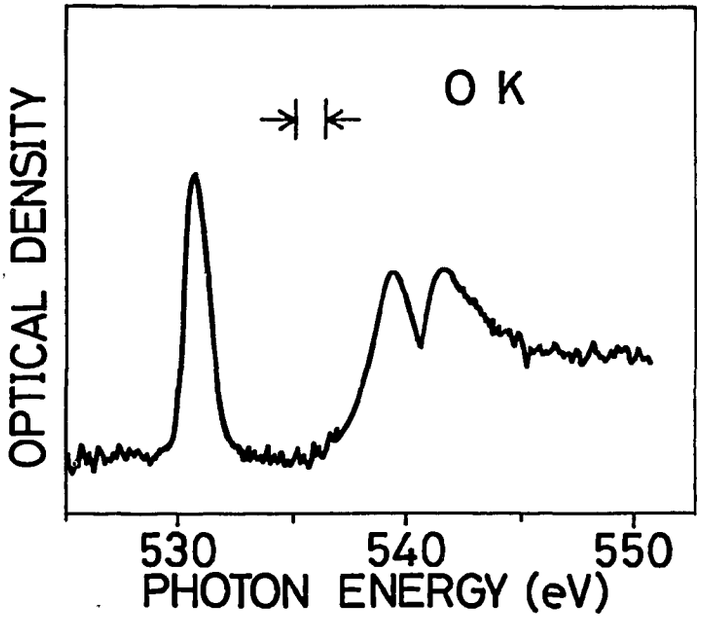

Fig. 10 Absorption spectrum of the O K edge for 0.8 Torr oxygen gas.

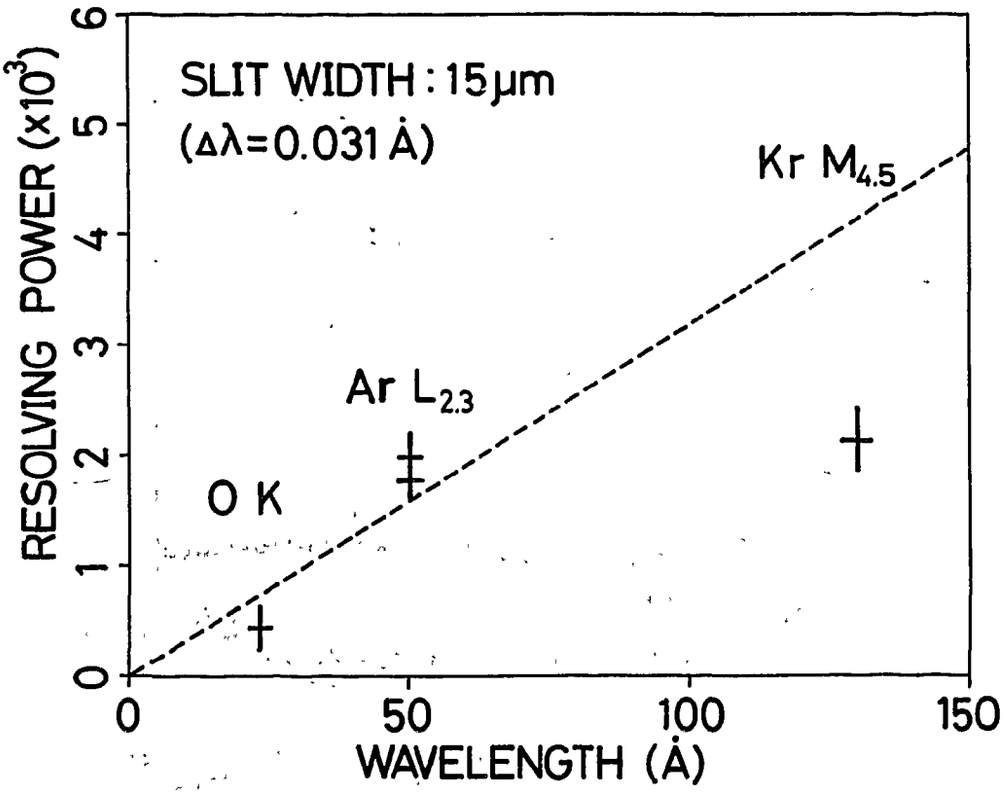

Fig. 11 Resolving power estimated from the FWHM of the absorption peaks b comparing with the electron-energy-loss spectra. The broken lin shows the calculated values.